

UDC 62.001

DOI: 10.15587/1729-4061.2023.293009

DEVELOPMENT OF FE-13.8CR-8.9MN ALLOY FOR STEEL BIOMATERIALS

Ratna Kartikasari

Corresponding Author

Doctor of Mechanical Engineering, Professor*

E-mail: ratna@itny.ac.id

Adi Subardi

Doctor of Materials Science and Engineering, Associate Professor*

Rivan Muhfidin

Master of Materials Science and Engineering, Assistance Professor*

Ihwanul Aziz

Bachelor of Engineering, Engineer

Center for Accelerator Science and Technology

National Nuclear Energy Agency of Indonesia (BATAN)

Babarsari str., Caturtunggal, Sleman, Yogyakarta, Indonesia, 55281

Marwan Effendy

Doctor of Mechanical Engineering, Professor

Department of Mechanical Engineering

Universitas Muhammadiyah Surakarta

A. Yani str., Pabelan, Kartasura, Sukoharjo,

Jawa Tengah, Indonesia, 57169

Triyono

Doctor of Mechanical Engineering, Professor**

Kuncoro Diharjo

Doctor of Mechanical Engineering, Professor**

*Department of Mechanical Engineering

Institut Teknologi Nasional Yogyakarta

Babarsari str., Caturtunggal, Depok, Sleman, Indonesia, 55281

**Department of Mechanical Engineering

Surakarta State University

Ir. Sutami str., 36, Surakarta, Indonesia, 57126

Traumatic, osteoarthritic, tumoral, and congenital bone issues impact human lives and health. The next generation of bone implants is made from biodegradable materials, including Fe-based materials with superior mechanical properties and high biocompatibility. However, efforts to inhibit the risk of inflammation and bacterial infection due to the biological response and corrosion properties of metals are a significant challenge. This study aims to develop biomaterials based on Fe-Cr-Mn alloys to obtain superior physical and mechanical properties through plasma nitriding. Each sample was plasma-nitridated in a vacuum chamber at various temperatures of 250–450 °C for 3 hours at a pressure of 1.8 kPa. Several main tests were performed to investigate the effects of plasma nitriding, such as the chemical compositions of raw material, surface nitrogen contents, phase changes, thickness, hardness, and corrosion. Those parameters were then used to evaluate plasma nitriding's effectiveness, including observing the change in phenomena at each temperature treatment. The results indicated that forming the S phase on the surface of Fe-13.8Cr-8.9Mn alloy is a saturated solution of nitrogen in γ -Fe, where the nitrogen content on the surface increases with increasing nitriding temperature. The layer's surface hardness is uniform across its whole thickness, which reduces as the grade of raw material passes through the nitride layer. The highest hardness at a nitriding temperature of 450 °C reached 625.3 VHN. The findings showed that the corrosion rate decreased significantly, reaching the lowest value, 0.0018 mm/year, at a plasma nitriding temperature of 450 °C. Plasma nitriding could enhance the physical and mechanical properties of Fe-Cr-Mn alloy

Keywords: plasma nitriding, Fe-13.8Cr-8.9Mn alloy, biomaterials, surface hardness, corrosion resistance, bone implant

Received date 09.10.2023

Accepted date 11.12.2023

Published date 27.12.2023

How to Cite: Kartikasari, R., Subardi, A., Muhfidin, R., Aziz, I., Effendy, M., Triyono, Diharjo, K. (2023). Development of Fe-13.8Cr-8.9Mn alloy for steel biomaterials. *Eastern-European Journal of Enterprise Technologies*, 6 (12 (126)), 6–15. doi: <https://doi.org/10.15587/1729-4061.2023.293009>

1. Introduction

The biomaterials field is an exciting issue since artificial bone implants can improve living standards and prolong human life [1]. To date, bone implant procedures have significantly improved the quality of life. Artificial bone can be a supporting structure to sustain mechanical loads, support fractures, or replace all permanently fractured bones [2]. Synthetic implants with strong biocompatibility and outstanding mechanical properties have become preferred. However, most artificial implants still do not successfully heal damaged bone, mainly when those injuries are caused by tumors, inflammation, or bacterial infections [3–6]. In

order to enhance bone healing and beneficial therapeutic effects, improving the practical properties of biomaterials is crucial.

Many studies have shown that functionalizing biomaterials is one of the most efficient to address these issues and enhance bone healing and treatment effectiveness [7–14]. Because of their inexpensive cost, nearly unlimited availability, and excellent mechanical behavior, Fe and its alloys are among the most desirable materials. However, the high rate of adverse side effects, such as corrosiveness, poor biocompatibility, and tissue irritation, results in few applications despite its good manufacturability [15]. The Fe is a crucial trace element for living and is involved in the produc-

tion of hemoglobin, DNA synthesis, and many other physiological processes like oxygen transfer [16, 17]. Moreover, preliminary research on using Fe as biodegradable implant materials in vivo shows no apparent indications of toxicity or an inflammatory response [18].

The biological compatibility system with the human organism is fundamental in developing biomaterials. Orthopedic and prosthetic implant devices are frequently constructed using austenitic stainless steel, AISI 316L. This material is economically viable and exhibits durable mechanical properties. Compared to other materials, the fabrication process for this material is relatively simple [19]. Therefore, research to improve mechanical properties and excellent corrosion resistance becomes relevant because it aims to create biomaterials that are adaptive to body tissues and non-toxic.

2. Literature review and problem statement

Biomaterial implants have been widely applied in many parts of the human body, aiming at structural repair. The implant material is expected to meet the application requirements, including corrosion resistance, high ductility and toughness, and good bone and surrounding tissue adaptation. Therefore, metal implant biomaterials are more durable and applicable than conventional ceramic and polymer biomaterials [20]. Ceramic-based bioactive materials are combined oxides (SiO_2 , CaO , MgO , P_2O_5 , etc.) that stimulate bone composition. Generally, the main elements consist of Ca and P, and the Ca/P ratio must be controlled (bone Ca/P ratio is 1.67). This bioactive material has obstacles in medical applications, especially load-bearing implants, where this material is brittle and weak [21]. The fracture toughness of this material is very low, namely below $1 \text{ Mpa}\cdot\text{m}^{1/2}$ while that of cortical bone reaches $2\text{--}10 \text{ Mpa}\cdot\text{m}^{1/2}$ [22]. A significant weakness of ceramic biomaterials is that they are brittle and tend to be damaged by tensile or cyclic loads so that the bone's function is to bear the load. In general, the essential mechanical properties of ceramics include:

- 1) weak resistance to tensile loads;
- 2) high hardness;
- 3) low plasticity, and very low fracture toughness in contrast to metal alloys having ductile behavior [23].

The KIC coefficient indicates the stress value for pre-existing cracks in standard specimens so they can propagate quickly when the specimen receives tension. The KIC value of ceramics is relatively low, in the range of $2\text{--}4 \text{ MPa}\cdot\text{m}^{1/2}$, smaller than that of metals [24]. The resistance of ceramics to tensile loads is much smaller than their resistance to compressive loads. Polymer implants have poor tribological properties thereby reducing durability. Polymer implants also face problems because they easily absorb water and protein [2]. Thus, ceramics and polymers are unsuitable as bone tissue implants when receiving tensile and repetitive loads. However, polymers and ceramics still have excellent abilities to implant parts of the human body that do not receive tensile or repetitive loads, including the ear bones.

The main obstacles to metal implant biomaterials are the metal surface releasing ions, the high elastic modulus, and the metal surface reacting chemically with bodily acids and enzymes. These conditions can result in toxicity, oxidative stress shielding, or bone resorption, resulting in implant failure. Consequently, vascularization of the surrounding body tissue can cause infection and implant failure [25].

Stainless steel (SS) implants are most commonly used as medical devices due to their low cost and relatively easy fabrication. Nickel-SS shows excellent mechanical properties and an easy hardening process. Compared to other conventional stainless steels, stainless steel in the annealed condition has higher strength in implant fabrication. It is expected to provide fabrication opportunities that produce more applicable and resilient implant materials tailored to the needs of specific patients [26].

Currently, austenitic stainless steel, AISI 316L, is the choice and is widely implemented as a synthetic material as a biomaterial for orthopedic and prosthetic implants.

Various studies show that this material has superior mechanical capabilities, fabrication is simpler than others and is cheaper than bio-based materials. Compared to other stainless steels, CrNx-coated 316L stainless steel under 4 A filament current has lower interfacial contact resistance (ICR) values in the measured compaction force range [19]. After the surface of the 316L SS sample was modified through the magnetically electropolished (MEP) process, the results showed a decreased corrosion rate. Magneto-electropolishing techniques to modify the composition of metal surface films can improve the 316L SS biomaterials [27]. Over the course of 13 months, the in vivo degrading performance of two Fe-based alloys (Fe-10Mn-1Pd and Fe-21Mn-0.7C-1Pd) and pure Fe was examined in a live mouse model. Results showed no local toxicity postoperatively, and no clinical abnormalities were tested [28].

However, some problems arise, namely a higher modulus of elasticity than that, which impacts the shielding effect stress, which can slow down bone healing. Another problem is that stainless steel is less resilient in a wet body environment, causing higher corrosive potential and wear and releasing toxic substances in the human body.

A study showed that Ni-free high nitrogen austenitic SS with higher strength and ductility, combined with nitrogen to increase corrosion resistance, is an acceptable alternative [29]. According to the Schaeffler diagram, several elements, such as N, Mn, and Co, could replace Ni. Nickel-free stainless steel with a high nitrogen content is a viable alternative to conventional medical stainless steel [26]. Carbon+nitrogen in the alloy can increase the metallic character of the bonds between atoms, resulting in a bulk modulus comparable to the modulus of pure iron [30]. Controlling the relative proportion of carbon (C/N) in C+N-added alloys can provide an outstanding combination of mechanical characteristics and corrosion resistance [31].

The alloy containing carbon and nitrogen has two effects when combined:

- 1) the free electrons concentration increases;
- 2) the critical interstitial content shifts towards higher values [30].

Deformation twinning emerged as the predominant plastic deformation method as the C fraction rose, suppressing the strain-induced $\gamma \rightarrow \epsilon$ martensitic transition [31]. Adding carbon increases the local corrosion resistance in chloride environments, which is affected by increasing the passive film stability [32].

Massive research has been performed to improve the capabilities of traditional CrNi stainless steel as a biomaterial. Various studies show that new stainless steels have greater muscle strength [26], ductility, and impact toughness [30, 33], as well as more extended fatigue [34]. Chromium and manganese additions to steel simultaneously strengthen

and stabilize the austenitic phase by increasing its solubility in nitrogen [30, 35].

Metal biomaterials used in implant devices include stainless steel, commercially pure titanium, cobalt-chromium alloy, and their alloys. Stainless steel low cost compared to other metals has led to its widespread application as a biomaterial. In addition, stainless steel has high mechanical qualities and corrosion resistance [36]. On the other hand, those materials may cause side effects, such as less biocompatibility, lack of affinity for cells and tissues, corrosion fatigue, and fractures. Some fractures are generally caused by various types of corrosion, such as fissures, intergranular, pits, and frets [37]. Furthermore, fretting debris and corrosion by products are toxic to living tissue. The toxicity problem, in particular, has a role in other issues, such as allergy symptoms and inflammation [38, 39]. These problems are associated with the nickel contents of austenitic stainless steel.

Plasma nitriding has more advantages besides making high cycle fatigue ranges stronger at lower cyclic loads. Extended fatigue life in certain types of steel is caused by plasma nitriding's internal compressive stresses [40]. A recent study found that plasma nitriding improves stainless steel's resistance to wear and corrosion [41], but only if the highest treatment temperature, as determined by electron probe microanalysis (EPMA), is lower than 475 °C [42]. Nitrogen plays a crucial role in forming austenite and has been effectively used to substitute nickel, substantially enhancing steel's mechanical characteristics and corrosion resistance.

It has also been found that adding nitrogen increases the hardness. Nitrogen enhances the solid solution hardening and dislocation processes, which together cause austenitic stainless steels to become harder [43]. Low-temperature nitriding increases austenitic stainless steel's surface hardness and corrosion resistance through surface engineering. Creating a supersaturated solid nitrogen solution, also known as the S phase, in the deformed and enlarged austenite lattice is usually considered an improvement [44]. The processing temperature should be kept below 450 °C to prevent the development of chromium nitride. However, a study noted that the alloy composition and nitriding conditions significantly impact the properties of the changed surface layer [45].

Plasma nitriding provides numerous benefits for steel, including increased resistance to pitting corrosion. In this situation, the plasma-nitrided material's resistivity has increased considerably. Increased resistance to pitting corrosion is primarily attributable to nitriding at a high nitrogen partial pressure [41]. Plasma nitriding could produce new phases with improved mechanical and technical qualities. This layer has five times the microhardness of the untreated material, and even at higher loads, wear is significantly reduced. The friction coefficient of plasma-nitrided austenitic steel is lower than that of untreated steel and ferritic and austenitic steel.

The plasma nitriding procedure in the study implants the N element onto the surface of the Fe-Cr-Mn alloy rather than adding it during the alloying phase of smelting. The plasma nitriding technique is commonly used to improve surface qualities like hardness, wear, and corrosion resistance [45]. Further research, a plasma nitriding is carried out on the Fe-13.8Cr-8.9Mn alloy to develop Ni-free steel biomaterials. In applying Ni-free biomaterials, N elements are generally added to steel materials as a substitute for Ni when smelting into Fe-Cr-N steel alloys. In this study, Ni is replaced by Mn, which is relatively cheaper and abundant. Meanwhile,

surface diffusion of N is used in plasma nitriding to boost the Fe-Cr-Mn alloy's hardness quality and corrosion resistance.

The references mentioned above show that new biomaterials based on nickel-free stainless steel are an option to avoid the negative impact of AISI 316L stainless steel on human body tissue. The newly designed biomaterial compound is expected to have high mechanical capability and high corrosion resistance compared to pure metal.

3. The aim and objectives of the study

The aim of the study is to develop an Fe-13.8Cr-8.9Mn alloy as a biomaterial bone implant with plasma nitriding treatment at various temperature variations between 250 to 450 °C.

To achieve this aim, the following objectives are accomplished:

- investigation of the microstructure on the surface of the Fe-13.8Cr-8.9Mn alloy;
- investigation of the hardness of Fe-13.8Cr-8.9Mn alloy;
- investigation of the physical properties of corrosion resistance.

4. Materials and Experimental Part

4. 1. Object and hypothesis of the study

The object of this research is to obtain artificial implants with excellent mechanical properties and biocompatibility. Hardness testing determines the mechanical properties of the implant material, while biocompatibility testing is carried out, one of which is corrosion testing on the implant material. After receiving a biomaterial implant, body tissue will be free from toxins if the implant material has excellent corrosion resistance properties and is even corrosion-free. Meanwhile, the hypothesis of this research is that increasing the plasma nitriding temperature can increase the hardness and corrosion resistance of the Fe-13.8Cr-8.9Mn steel alloy. In this work, several tests, including corrosion, surface hardness, and microstructure, have been conducted to assess the surface properties of the Fe-13.8Cr-8.9Mn alloy following plasma nitriding.

4. 2. Materials

This study used the raw material of Fe-13.8Cr-8.9Mn alloy, with chemical composition as presented in Table 1. The ASTM E2209 standard test method was utilized to conduct the tests on this composition using a Baird FSQ Foundry Spectrovac Spectrometer. The illustration of the specimen before-and-after plasma nitriding is given in Fig. 1.

Table 1

The chemical composition of Fe-13.8Cr-8.9Mn alloy

Elements	Fe	Cr	Mn	C	P	S	Si	Mo	Ni
% weight	Balance	13.79	8.90	0.12	0.53	0.01	0.38	0.10	0.48

The chemical compositions of the Cr and Mn alloy elements are consistent with the ratios applied to these specimens. In addition, the following elements were detected as C, P, S, Si Mo, and Ni in relatively small amounts overall, reaching 1.52 %. In this work, adding Nitrogen during the plasma nitriding process to the Fe-13.8Cr-8.9Mn alloy produces austenitic stainless steel with increased hardness,

strength, and corrosion resistance. Manganese (Mn) elements play a role in increasing the solubility of Nitrogen and function to stabilize the austenitic microstructure. Mn is an essential human body element and, therefore, biocompatible.

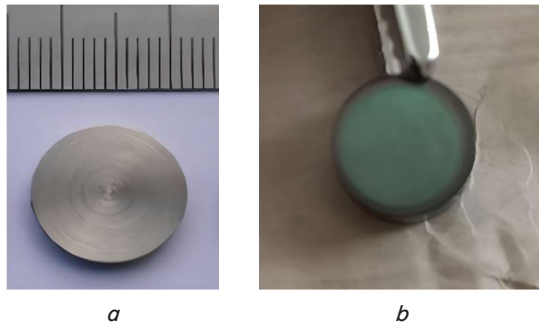


Fig. 1. Specimens: *a* – raw material; *b* – after plasma nitriding at 450 °C

Stainless steels containing more than 12 % Cr and low or even Ni-free Ni elements provide excellent corrosion resistance and high material strength [46]. As previously reported, the biocompatibility of Fe-18Cr-22Mn-0.65N austenitic stainless steel was very satisfactory. In vitro cell culture and cell proliferation (MTT) tests were performed on these specimens compared to SS 316L. Average % proliferation of MG-63 cells increased from ≈ 88 % for Un-USP to 98 % (USP samples 3-2) and 105 % (USP samples 2-2) in vivo rabbits without allergic reactions [47]. High corrosion resistance in the Fe-13.8Cr-8.9Mn alloy will be beneficial in the long term because toxic bone tissue can be minimized.

4. 3. Experiments and Characterization

In the experiments, a cylindrical Fe-13.8Cr-8.9Mn alloy steel with a diameter of 14 mm was prepared by metal cutting into plasma nitriding samples with 5 mm height for the nitriding process. Further, the specimen surfaces were smoothed using sandpaper in various mesh at 400, 800, 1000, 1500, and 2000 and polished by the diamond paste using a polishing machine. Samples were cleaned using an ultrasonic cleaner to remove dirt and oil, followed by surface drying. The nitriding treatment utilized a plasma nitriding apparatus with a metal vacuum chamber, as in Fig. 2. It had a temperature controller, a high-voltage DC system, a nitrogen gas input, and a vacuum facility.

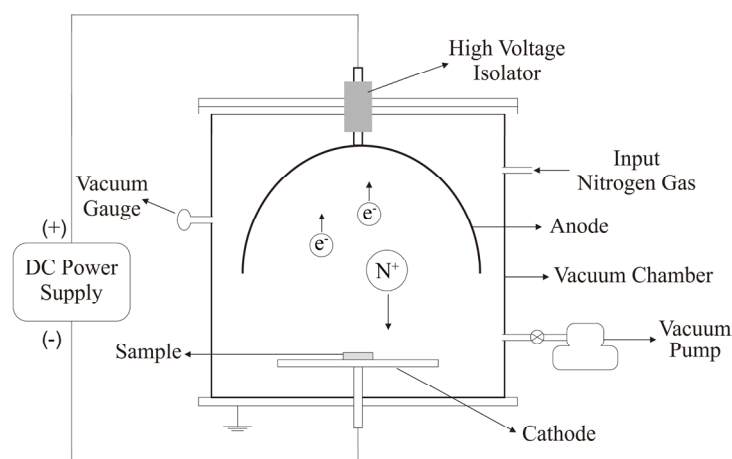


Fig. 2. The schematic of the plasma nitriding apparatus

The nitriding procedure was completed in 3 hours at 250 °C, 300 °C, 350 °C, 400 °C, and 450 °C and 1.8 kPa of pressure. Fe-Cr-Mn alloy's surface N content and thickness were evaluated using JEOL 7000 EDS equipment and CuK radiation, while phases were investigated utilizing a 2 kW XRD apparatus, Rigaku Multiflex. Hardness Tester DIA Testory micro-Vickers method based on ASTM E384 was used to evaluate the hardness distribution of the Fe-Cr-Mn alloy's transverse surface.

The Corrtest CS310 was used in a 9 % NaCl solution for a corrosion test. Several analyses were carried out to compare types, sizes, shapes, and microstructural patterns based on a range of plasma nitriding temperatures.

5. Result of Fe-13.8Cr-8.9Mn Alloy Performance Test

5. 1. Investigation of the microstructure on the surface of the Fe-13.8Cr-8.9Mn alloy

An experimental study has been performed on the Fe-13.8Cr-8.9Mn alloy for plasma nitriding at temperatures between 250 °C and 450 °C for nickel-free steel biomaterials. The primary findings and an expanded analysis are shown below.

Fig. 3 shows the microstructure results of the Fe-13.8Cr-8.9Mn alloy using a scanning electron microscope (SEM). The alloy has a balanced austenitic and ferrite structure. This fact indicates the presence of Cr as a stabilizer for the ferrite structure (α) and Mn as a stabilizer for austenite (γ), as found by another researcher [48]. It was discovered that the temperature during the nitriding process affects the thickness of the S phase layer. The plasma nitriding process produces a layer thicker than the base material between 250 °C and 450 °C [40].

Fig. 4 indicates the relationship between the S layer thickness on the surface of the Fe-13.8Cr-8.9Mn alloy and the plasma nitriding temperature. The S layer thickness is 6.142 μm at 250 °C, and it increases to 7.571 μm at 450 °C. It means an increase of 23.27 % from 250 °C to 450 °C. Interestingly, there is a significant increase of up to 11.64 % from 250 °C to 300 °C. Furthermore, there is a substantial increase from 400 °C to 450 °C.

Fig. 5 shows the observed phenomena from the EDS test data; the composition changes following plasma nitriding at temperatures ranging from 250 °C to 450 °C. The Fe-13.8Cr-8.9Mn alloy raw material contains Cr, Mn, and C elements. No N elements were identified from the raw material. The alloying elements in the specimens correspond to the element ratio estimations used to prepare the samples.

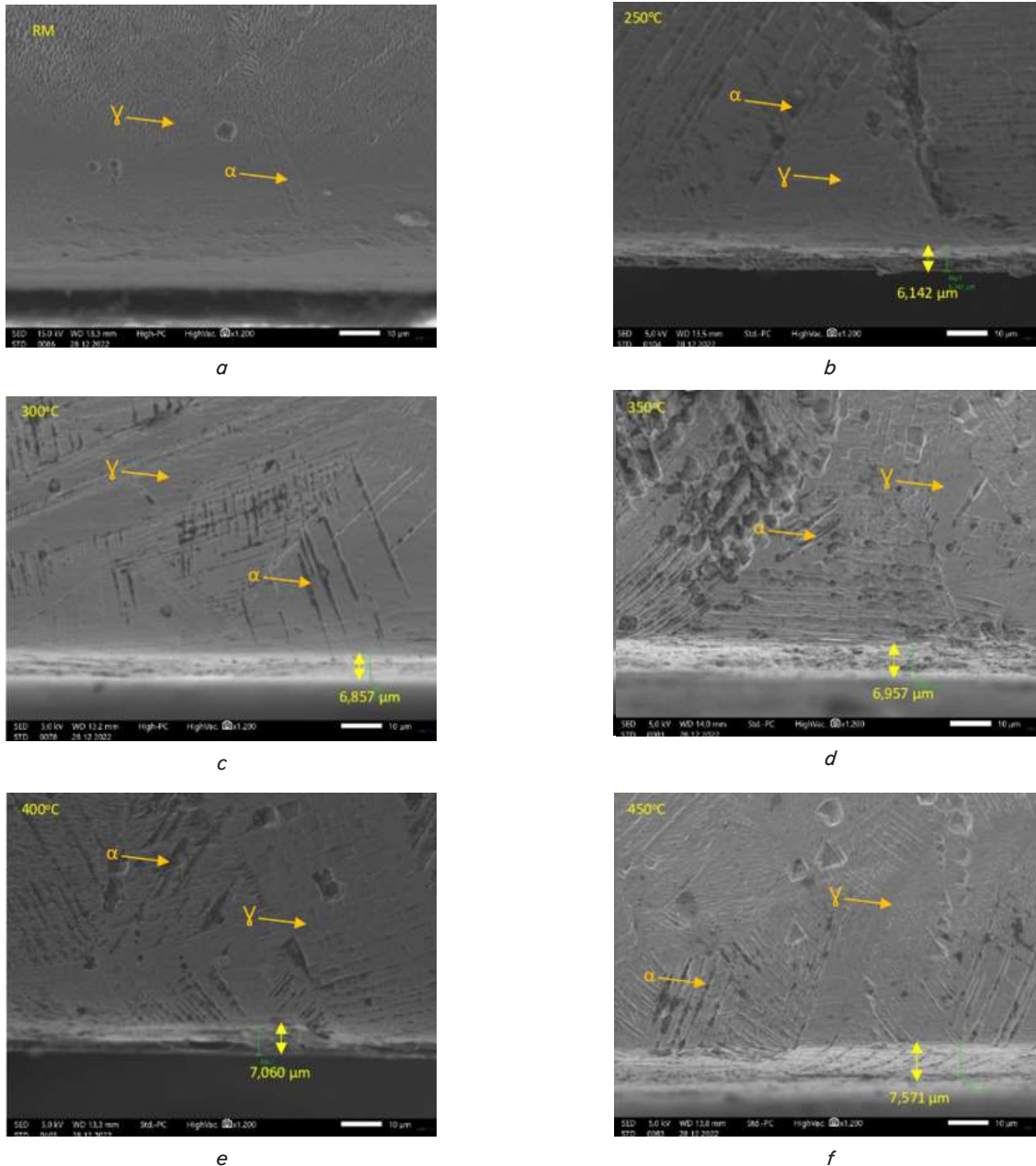


Fig. 3. The Cross-Sectional micrograph of specimens before and after plasma nitriding: *a* – raw material; *b* – 250 °C; *c* – 300 °C, *d* – 350 °C; *e* – 400 °C; *f* – 450 °C

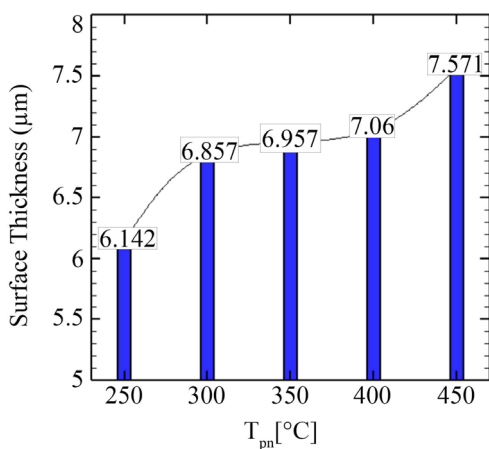


Fig. 4. The surface thickness of Fe-13.8Cr-8.9Mn alloy after plasma nitriding

After the plasma nitriding, the N elements exist, as shown in Fig. 6. It implies that the diffusion of N atoms to the surface of the Fe-13.8Cr-8.9Mn alloy increases as the plasma nitriding temperature rises. The increase in element N during plasma nitriding from 250 °C to 400 °C was 8.4 %.

There was a significant increase in element N during plasma nitriding at 450 °C by 13.5 %. Based on Fig. 7, there are various phases in Fe-Cr-Mn alloy before and after the plasma nitriding. In the raw material Fe-13.8Cr-8.9Mn alloy, the austenite (γ) Fe-Mn phase (111) and Cr carbides (CrC) in the (111) plane are identified.

The peaks that can be identified in the sample a crystal phase is formed. High peak intensity indicates a high percentage of FeN elements. The elements CrN and CrC have not been detected, this is because the raw samples were not treated and were at room temperature. The CrC element was detected after the sample was heat treated.

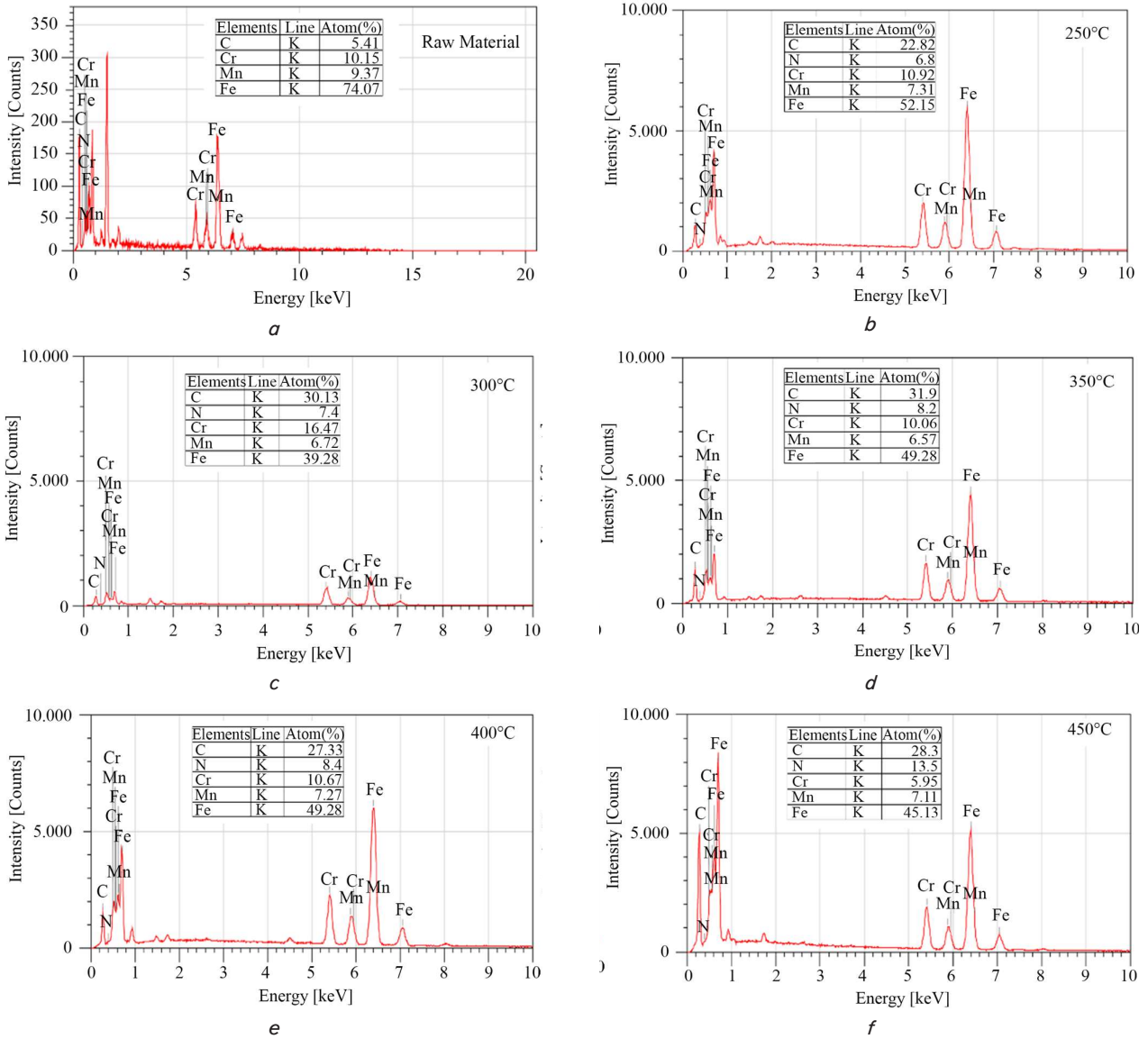


Fig. 5. The EDS of Fe-13.79Cr-8.9Mn alloy: a – raw material; b – 250 °C; c – 300 °C, d – 350 °C; e – 400 °C; f – 450 °C

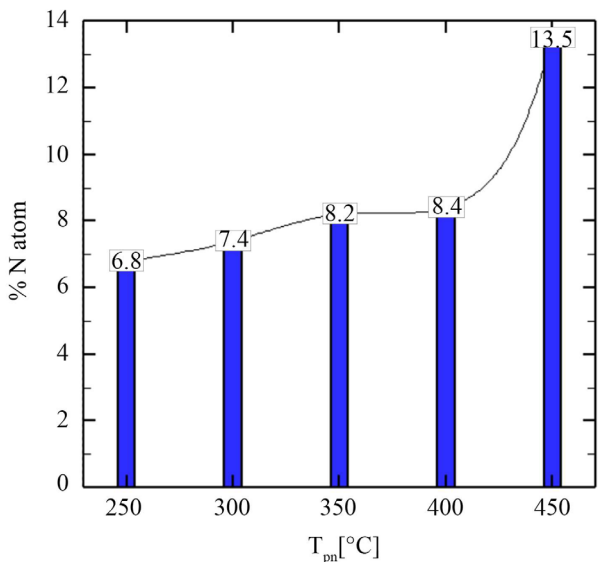


Fig. 6. The N percentage on the surface of Fe-13.8Cr-8.9 Mn alloy after plasma nitriding

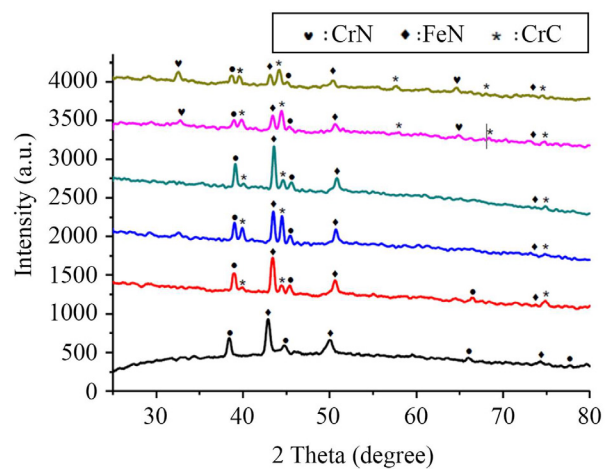


Fig. 7. The XRD results of Fe-13.79Cr-8.9 Mn alloy

5. 2. Investigation of the hardness of Fe-13.8Cr-8.9Mn alloy

Based on the measurement, the rate of increase in hardness values is directly proportional to the plasma nitriding

temperature in the interval 250 °C to 450 °C as shown in Fig. 8. Elevating the plasma nitriding temperature enhances the toughness, with an average hardness increase of 22 %. The hardness increases three times at the nitriding temperature of 450 °C, which amounts to 625.3 VHN. From the variations in plasma nitriding temperature applied when testing specimens, important information is obtained about the optimal limit of mechanical strength of the material. According to this study, plasma nitriding modifies the nitride formation on the material's surface [49].

The Vickers hardness test is equipped with a program system and a digital and metallurgy microscope. Test data shows differences in hardness values specimens affected by plasma nitriding temperature. Table 2 indicates the hardness of Fe-13.8Cr-8.9Mn alloy after plasma nitriding up to a temperature of 450 °C.

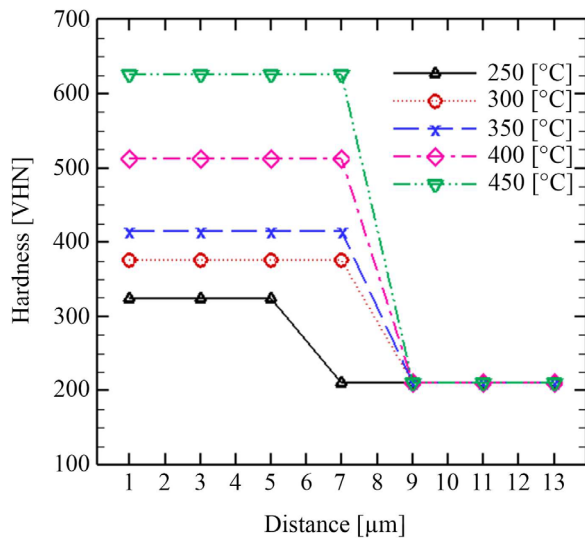


Fig. 8. The hardness distribution of Fe-13.8Cr-8.9Mn alloy after plasma nitriding

Table 2
The hardness of Fe-13.8Cr-8.9Mn alloy after plasma nitriding

Nitriding temperature (°C)	Raw material (RM)	250	300	350	400	450
Hardness (VHN)	210.2	324.6	375.4	415.3	512.4	625.3

The raw material hardness value at room temperature is 210.2 VHN, while the hardness value at plasma nitriding temperatures of 250 °C, 350 °C, and 450 °C reaches 324 VHN, 415.3 VHN, and 625 VHN, respectively. In this case, adding temperature can increase the hardness of the Fe-13.8Cr-8.9Mn steel alloy. In this case, heating the steel to the austenite temperature will increase carbon solubility, so the carbon will dissolve in the alloy.

5. 3. Investigation of the physical properties of corrosion resistance

Table 3 shows the corrosion rate of Fe-13.8Cr-8.9Mn alloy after plasma nitriding temperature between 250 °C and 450 °C. The raw material alloy has a corrosion rate of 0.0033 mm/yr from measurement. This corrosion rate is in a particular category. The presence of the Cr element, which forms an immune Cr oxide layer on the surface, triggers this remarkable corrosion rate.

Table 3

The corrosion rate of Fe-13.8Cr-8.9Mn alloy after plasma nitriding

Nitriding temperature (°C)	250	300	350	400	450
Corrosion rate (mm/yr)	0.0031	0.0025	0.0021	0.0019	0.0018

The corrosion rate data shows that samples with a plasma nitriding temperature of 450 °C achieved the lowest corrosion rate. This phenomenon can be caused by forming a nitride layer or austenite expansion, which increases corrosion resistance.

6. Discussion of results of Fe-13.8Cr-8.9Mn Alloy Performance Test

This study focused on the mechanical and physical properties and did not investigate the fatigue properties of Fe-13.8Cr-8.9Mn alloy steel. Fatigue testing can describe material performance under actual working conditions. However, hardness can reflect the fatigue properties of alloy steel as a requirement for biomaterial implants. The discussion has been organized by answering the research objectives including [1] investigating the microstructure on the surface of the sample, [2] investigating the hardness of the sample after nitriding, and [3] sample testing after plasma nitriding temperature on the corrosion rate of Fe-13.8Cr-8.9Mn alloy steel.

Fig. 3 shows the ferrite structure spreads between the grains of austenite structure, with uniform size. The alloy belongs to the duplex stainless-steel category. After the plasma nitriding process at a temperature of 250–450 °C, a thin layer of the white color is formed on the surface. Li defines it as the S phase [50]. The S phase, a saturated solution of N in γ-Fe, is often referred to as expanded austenite. As previously reported, it has metastable characteristics [51].

The surface morphology of the Fe-Cr-Mn alloy fracture shows no visible boundary layer between the S phase and the substrate. Nitrogen atoms diffuse to the surface of the Fe-13.8Cr-8.9Mn alloy and occupy interstitial positions in the austenite structure during the plasma nitriding process: These findings are similar to those of other researchers [52]. It indicates that the S phase is the zone of nitrogen atom diffusion in the plasma nitriding of Fe-13.8Cr-8.9Mn alloy without an intrinsic interface. N atoms in the interstitial γ-Fe of the Fe-13.8Cr-8.9Mn alloy are soluble due to elemental Mn, as discovered by both researchers [30, 53].

Fig. 4 indicates that the plasma nitriding temperature is essential to the S layer thickness. It correlates to the energy of the N atom to diffuse to the surface of the Fe-13.8Cr-8.9Mn alloy through the interstitial position in the FCC (γ-Fe) structure. The higher the temperature, the greater the distance between atoms. The N atom with tremendous energy enters the γ-Fe interstitial position more quickly, as found in the reference [41]. The plasma nitriding process increases the spacing between particles by causing the atoms to vibrate and shift from their stable state, as exhibited in Fig. 5. The distance between Fe and Mn atoms (lattice) in the FCC structure (γ-Fe) is wider with higher plasma nitriding temperature. As in this reference, it allows more N atoms to occupy interstitial positions between Fe and Mn atoms [54].

After the plasma nitriding, the highest peak (111) is recognized as the S phase, a supersaturated N solution in Fe, as presented in Fig. 7. According to this reference, the lower

peak (111) is identified as the nitride-Fe (FeN) phase [46]. The CrN compound is found in small amounts on the surface of the Fe-13.8Cr-8.9Mn alloy.

Fig. 8 shows that the increase in surface N content and the formation of the S phase contribute significantly to the alloy's surface hardness increasing over time. Fig. 8 also illustrates the distribution of hardness of the Fe-13.8Cr-8.9Mn alloy following nitriding. The Fe-13.8Cr-8.9Mn alloy has uniform hardness along the nitride layer (S phase) at varying thicknesses. This consistent number indicates the homogeneity of this layer. After plasma nitriding, the corrosion rate decreased to the lowest value, 0.0018 mm/yr, at 450 °C, as presented in Table 3. This decrease, up to 45 %, is very significant. In this case, apart from Cr being able to self-repair in a corrosive environment, there is a role for nitride compounds and the formation of the S phase on the surface.

This research is focused on the mechanical and physical field properties and has not examined the fatigue properties and the fracture toughness of Fe-13.8Cr-8.9Mn alloy. The Material performance under actual operating conditions can be explained by fatigue testing. However, testing for tensile strength and hardness might reveal fatigue characteristics of alloy steel. Additionally, further research and development are needed to improve the performance of Fe-13.8Cr-8.9Mn steel alloys. Heat treatment via quenching is a conventional technique that can be applied to increase the surface hardness of steel alloys. With this technique, hardness, ductility, and wear resistance can be increased.

7. Conclusions

1. The plasma nitriding causes the change of N elements on the alloy surface. The S phase appears on the surface of Fe-13.8Cr-8.9Mn alloy due to N saturation in γ -Fe.

2. The surface hardness appears uniform over the entire thickness of the layer, which decreases as the raw materi-

al passes through the nitride layer. The average increase in hardness is 22 %, and the maximum hardness reaches 625.3 VHN at a plasma nitriding temperature of 450 °C.

3. The corrosion resistance of Fe-Cr-Mn alloys could be increased by up to 0.0018 mm/year using plasma nitriding up to 450 °C. Therefore, the Fe-Cr-Mn alloy with plasma nitriding treatment can be projected to be an alternative for steel biomaterials. The lowest corrosion rate reached 0.0018 mm/year at a plasma nitriding temperature of 450 °C.

Conflict of interest

The authors declare that no conflicts of interest concerning this research, whether financial, personal, authorial or otherwise, that could influence the research and the results presented in this paper.

Financing

The study was funded by The Ministry of Research, Technology and Higher Education, The Republic of Indonesia "Regular Fundamental Research Grants" under Decree number: 04/ITNY/LPPMI/Pen.DRTPM/PFR/VII/2023.

Data availability

Data will be made available on reasonable request.

Use of artificial intelligence

The authors confirm that they did not use artificial intelligence technologies when creating the current work.

References

- Bandyopadhyay, A., Mitra, I., Goodman, S. B., Kumar, M., Bose, S. (2023). Improving biocompatibility for next generation of metallic implants. *Progress in Materials Science*, 133, 101053. doi: <https://doi.org/10.1016/j.pmatsci.2022.101053>
- Szczęśny, G., Kopec, M., Politis, D. J., Kowalewski, Z. L., Łazarski, A., Szolc, T. (2022). A Review on Biomaterials for Orthopaedic Surgery and Traumatology: From Past to Present. *Materials*, 15 (10), 3622. doi: <https://doi.org/10.3390/ma15103622>
- Zhang, L., Yang, G., Johnson, B. N., Jia, X. (2019). Three-dimensional (3D) printed scaffold and material selection for bone repair. *Acta Biomaterialia*, 84, 16–33. doi: <https://doi.org/10.1016/j.actbio.2018.11.039>
- Zhao, C., Liu, W., Zhu, M., Wu, C., Zhu, Y. (2022). Bioceramic-based scaffolds with antibacterial function for bone tissue engineering: A review. *Bioactive Materials*, 18, 383–398. doi: <https://doi.org/10.1016/j.bioactmat.2022.02.010>
- Ma, H., Feng, C., Chang, J., Wu, C. (2018). 3D-printed bioceramic scaffolds: From bone tissue engineering to tumor therapy. *Acta Biomaterialia*, 79, 37–59. doi: <https://doi.org/10.1016/j.actbio.2018.08.026>
- Prestat, M., Thierry, D. (2021). Corrosion of titanium under simulated inflammation conditions: clinical context and in vitro investigations. *Acta Biomaterialia*, 136, 72–87. doi: <https://doi.org/10.1016/j.actbio.2021.10.002>
- Armiento, A. R., Hatt, L. P., Sanchez Rosenberg, G., Thompson, K., Stoddart, M. J. (2020). Functional Biomaterials for Bone Regeneration: A Lesson in Complex Biology. *Advanced Functional Materials*, 30 (44). doi: <https://doi.org/10.1002/adfm.201909874>
- Wang, X., Rivera Bolanos, N., Jiang, B., Ameer, G. A. (2019). Advanced Functional Biomaterials for Stem Cell Delivery in Regenerative Engineering and Medicine. *Advanced Functional Materials*, 29 (23). doi: <https://doi.org/10.1002/adfm.201809009>
- Park, J., Lee, S. J., Jung, T. G., Lee, J. H., Kim, W. D., Lee, J. Y., Park, S. A. (2021). Surface modification of a three-dimensional polycaprolactone scaffold by polydopamine, biomineralization, and BMP-2 immobilization for potential bone tissue applications. *Colloids and Surfaces B: Biointerfaces*, 199, 111528. doi: <https://doi.org/10.1016/j.colsurfb.2020.111528>
- Wang, X., Xue, J., Ma, B., Wu, J., Chang, J., Gelinsky, M., Wu, C. (2020). Black Bioceramics: Combining Regeneration with Therapy. *Advanced Materials*, 32 (48). doi: <https://doi.org/10.1002/adma.202005140>

11. Sheng, X., Li, C., Wang, Z., Xu, Y., Sun, Y., Zhang, W. et al. (2023). Advanced applications of strontium-containing biomaterials in bone tissue engineering. *Materials Today Bio*, 20, 100636. doi: <https://doi.org/10.1016/j.mtbio.2023.100636>
12. Huang, D., Wang, J., Ren, K., Ji, J. (2020). Functionalized biomaterials to combat biofilms. *Biomaterials Science*, 8 (15), 4052–4066. doi: <https://doi.org/10.1039/d0bm00526f>
13. Wei, H., Cui, J., Lin, K., Xie, J., Wang, X. (2022). Recent advances in smart stimuli-responsive biomaterials for bone therapeutics and regeneration. *Bone Research*, 10 (1). doi: <https://doi.org/10.1038/s41413-021-00180-y>
14. Lee, S., Lee, J., Byun, H., Kim, S., Joo, J., Park, H. H., shin, H. (2021). Evaluation of the anti-oxidative and ROS scavenging properties of biomaterials coated with epigallocatechin gallate for tissue engineering. *Acta Biomaterialia*, 124, 166–178. doi: <https://doi.org/10.1016/j.actbio.2021.02.005>
15. Abdalla, S. S. I., Katas, H., Azmi, F., Busra, M. F. M. (2020). Antibacterial and Anti-Biofilm Biosynthesised Silver and Gold Nanoparticles for Medical Applications: Mechanism of Action, Toxicity and Current Status. *Current Drug Delivery*, 17 (2), 88–100. doi: <https://doi.org/10.2174/1567201817666191227094334>
16. Jia, P., Wang, Z., Zhang, Y., Zhang, D., Gao, W., Su, Y. et al. (2020). Selective sensing of Fe³⁺ ions in aqueous solution by a biodegradable platform based lanthanide metal organic framework. *Spectrochimica Acta Part A: Molecular and Biomolecular Spectroscopy*, 230, 118084. doi: <https://doi.org/10.1016/j.saa.2020.118084>
17. Gorejová, R., Haverová, L., Oriňáková, R., Oriňák, A., Oriňák, M. (2018). Recent advancements in Fe-based biodegradable materials for bone repair. *Journal of Materials Science*, 54 (3), 1913–1947. doi: <https://doi.org/10.1007/s10853-018-3011-z>
18. Carluccio, D., Xu, C., Venezuela, J., Cao, Y., Kent, D., Bermingham, M. et al. (2020). Additively manufactured iron-manganese for biodegradable porous load-bearing bone scaffold applications. *Acta Biomaterialia*, 103, 346–360. doi: <https://doi.org/10.1016/j.actbio.2019.12.018>
19. Xu, M., Kang, S., Lu, J., Yan, X., Chen, T., Wang, Z. (2020). Properties of a Plasma-Nitrided Coating and a CrN_x Coating on the Stainless Steel Bipolar Plate of PEMFC. *Coatings*, 10 (2), 183. doi: <https://doi.org/10.3390/coatings10020183>
20. Al-Shalawi, F. D., Mohamed Ariff, A. H., Jung, D.-W., Mohd Ariffin, M. K. A., Seng Kim, C. L., Brabazon, D., Al-Osaimi, M. O. (2023). Biomaterials as Implants in the Orthopedic Field for Regenerative Medicine: Metal versus Synthetic Polymers. *Polymers*, 15 (12), 2601. doi: <https://doi.org/10.3390/polym15122601>
21. Wang, D., Chen, C., Ma, J., Lei, T. (2007). Microstructure of yttrium calcium phosphate bioceramic coatings synthesized by laser cladding. *Applied Surface Science*, 253 (8), 4016–4020. doi: <https://doi.org/10.1016/j.apsusc.2006.08.036>
22. Chien, C. S., Liu, C. W., Kuo, T. Y., Wu, C. C., Hong, T. F. (2016). Bioactivity of fluorapatite/alumina composite coatings deposited on Ti₆Al₄V substrates by laser cladding. *Applied Physics A*, 122 (4). doi: <https://doi.org/10.1007/s00339-016-9788-1>
23. De Angelis, F., Sarteur, N., Buonvivere, M., Vadini, M., Šteffl, M., D'Arcangelo, C. (2022). Meta-analytical analysis on components released from resin-based dental materials. *Clinical Oral Investigations*, 26 (10), 6015–6041. doi: <https://doi.org/10.1007/s00784-022-04625-4>
24. Ritchie, R. O. (2021). Toughening materials: enhancing resistance to fracture. *Philosophical Transactions of the Royal Society A: Mathematical, Physical and Engineering Sciences*, 379 (2203), 20200437. doi: <https://doi.org/10.1098/rsta.2020.0437>
25. Katti, K. S. (2004). Biomaterials in total joint replacement. *Colloids and Surfaces B: Biointerfaces*, 39 (3), 133–142. doi: <https://doi.org/10.1016/j.colsurfb.2003.12.002>
26. Yang, K., Ren, Y. (2010). Nickel-free austenitic stainless steels for medical applications. *Science and Technology of Advanced Materials*, 11 (1), 014105. doi: <https://doi.org/10.1088/1468-6996/11/1/014105>
27. Hryniewicz, T., Rokosz, K., Filippi, M. (2009). Biomaterial Studies on AISI 316L Stainless Steel after Magnetoelectropolishing. *Materials*, 2 (1), 129–145. doi: <https://doi.org/10.3390/ma2010129>
28. Kraus, T., Moszner, F., Fischerauer, S., Fiedler, M., Martinelli, E., Eichler, J. et al. (2014). Biodegradable Fe-based alloys for use in osteosynthesis: Outcome of an in vivo study after 52weeks. *Acta Biomaterialia*, 10 (7), 3346–3353. doi: <https://doi.org/10.1016/j.actbio.2014.04.007>
29. Zhang, J., Zhai, B., Gao, J., Li, Z., Zheng, Y., Ma, M. et al. (2022). Plain metallic biomaterials: opportunities and challenges. *Regenerative Biomaterials*, 10. doi: <https://doi.org/10.1093/rb/rbac093>
30. Shanina, B. D., Gavriljuk, V. G., Berns, H. (2007). High Strength Stainless Austenitic CrMnN steels - Part III: Electronic Properties. *Steel Research International*, 78 (9), 724–728. doi: <https://doi.org/10.1002/srin.200706276>
31. Lee, T.-H., Ha, H.-Y., Hwang, B., Kim, S.-J., Shin, E. (2012). Effect of Carbon Fraction on Stacking Fault Energy of Austenitic Stainless Steels. *Metallurgical and Materials Transactions A*, 43 (12), 4455–4459. doi: <https://doi.org/10.1007/s11661-012-1423-y>
32. Ha, H. Y., Lee, T. H., Oh, C. S., Kim, S. J. (2009). Effects of Carbon on the Corrosion Behaviour in Fe-18Cr-10Mn-N-C Stainless Steels. *Steel Research International*, 80 (7), 488–492. doi: <https://doi.org/10.2374/SRI09SP032>
33. Gavriljuk, V. G., Shanina, B. D., Berns, H. (2008). A physical concept for alloying steels with carbon+nitrogen. *Materials Science and Engineering: A*, 481–482, 707–712. doi: <https://doi.org/10.1016/j.msea.2006.11.186>
34. Kang, J., Zhang, F. C., Long, X. Y., Yang, Z. N. (2014). Synergistic enhancing effect of N+C alloying on cyclic deformation behaviors in austenitic steel. *Materials Science and Engineering: A*, 610, 427–435. doi: <https://doi.org/10.1016/j.msea.2014.05.052>

35. Uggowitz, P. J., Magdowski, R., Speidel, M. O. (1996). High Nitrogen Steels. Nickel Free High Nitrogen Austenitic Steels. *ISIJ International*, 36 (7), 901–908. doi: <https://doi.org/10.2355/isijinternational.36.901>
36. Talha, M., Ma, Y., Lin, Y., Pan, Y., Kong, X., Sinha, O. P., Behera, C. K. (2019). Corrosion performance of cold deformed austenitic stainless steels for biomedical applications. *Corrosion Reviews*, 37 (4), 283–306. doi: <https://doi.org/10.1515/corrrev-2019-0004>
37. Gurappa, I. (2002). Characterization of different materials for corrosion resistance under simulated body fluid conditions. *Materials Characterization*, 49 (1), 73–79. doi: [https://doi.org/10.1016/s1044-5803\(02\)00320-0](https://doi.org/10.1016/s1044-5803(02)00320-0)
38. Chua, K., Khan, I., Malhotra, R., Zhu, D. (2021). Additive manufacturing and 3D printing of metallic biomaterials. *Engineered Regeneration*, 2, 288–299. doi: <https://doi.org/10.1016/j.engreg.2021.11.002>
39. Eliaz, N. (2019). Corrosion of Metallic Biomaterials: A Review. *Materials*, 12 (3), 407. doi: <https://doi.org/10.3390/ma12030407>
40. Menthe, E., Bulak, A., Olfe, J., Zimmermann, A., Rie, K.-T. (2000). Improvement of the mechanical properties of austenitic stainless steel after plasma nitriding. *Surface and Coatings Technology*, 133-134, 259–263. doi: [https://doi.org/10.1016/s0257-8972\(00\)00930-0](https://doi.org/10.1016/s0257-8972(00)00930-0)
41. Kartikasari, R., Effendy, M. (2021). Surface characterization of Fe–10Al–25Mn alloy for biomaterial applications. *Journal of Materials Research and Technology*, 15, 409–415. doi: <https://doi.org/10.1016/j.jmrt.2021.08.006>
42. Menthe, E., Rie, K.-T. (1999). Further investigation of the structure and properties of austenitic stainless steel after plasma nitriding. *Surface and Coatings Technology*, 116–119, 199–204. doi: [https://doi.org/10.1016/s0257-8972\(99\)00085-7](https://doi.org/10.1016/s0257-8972(99)00085-7)
43. Behjati, P., Kermanpur, A., Najafizadeh, A., Samaei Baghbadorani, H., Karjalainen, L. P., Jung, J.-G., Lee, Y.-K. (2014). Effect of Nitrogen Content on Grain Refinement and Mechanical Properties of a Reversion-Treated Ni-Free 18Cr-12Mn Austenitic Stainless Steel. *Metallurgical and Materials Transactions A*, 45 (13), 6317–6328. doi: <https://doi.org/10.1007/s11661-014-2595-4>
44. Adachi, S., Ueda, N. (2012). Formation of S-phase layer on plasma sprayed AISI 316L stainless steel coating by plasma nitriding at low temperature. *Thin Solid Films*, 523, 11–14. doi: <https://doi.org/10.1016/j.tsf.2012.05.062>
45. Borgioli, E., Galvanetto, E., Bacci, T. (2016). Low temperature nitriding of AISI 300 and 200 series austenitic stainless steels. *Vacuum*, 127, 51–60. doi: <https://doi.org/10.1016/j.vacuum.2016.02.009>
46. Kim, T., See, C. W., Li, X., Zhu, D. (2020). Orthopedic implants and devices for bone fractures and defects: Past, present and perspective. *Engineered Regeneration*, 1, 6–18. doi: <https://doi.org/10.1016/j.engreg.2020.05.003>
47. Kumar, C. S., Singh, G., Poddar, S., Varshney, N., Mahto, S. K., Podder, A. S. et al. (2021). High-manganese and nitrogen stabilized austenitic stainless steel (Fe–18Cr–22Mn–0.65N): a material with a bright future for orthopedic implant devices. *Biomedical Materials*, 16 (6), 065011. doi: <https://doi.org/10.1088/1748-605x/ac265e>
48. Yang, F., Song, R., Li, Y., Sun, T., Wang, K. (2015). Tensile deformation of low density duplex Fe–Mn–Al–C steel. *Materials & Design*, 76, 32–39. doi: <https://doi.org/10.1016/j.matdes.2015.03.043>
49. Godec, M., Donik, Č., Kocijan, A., Podgornik, B., Skobir Balantič, D. A. (2020). Effect of post-treated low-temperature plasma nitriding on the wear and corrosion resistance of 316L stainless steel manufactured by laser powder-bed fusion. *Additive Manufacturing*, 32, 101000. doi: <https://doi.org/10.1016/j.addma.2019.101000>
50. Li, X. Y. (2001). Joint Second Prize Low Temperature Plasma Nitriding of 316 Stainless Steel – Nature of S Phase and Its Thermal Stability. *Surface Engineering*, 17 (2), 147–152. doi: <https://doi.org/10.1179/026708401101517746>
51. Gontijo, L. C., Machado, R., Miola, E. J., Casteletti, L. C., Alcântara, N. G., Nascente, P. A. P. (2006). Study of the S phase formed on plasma-nitrided AISI 316L stainless steel. *Materials Science and Engineering: A*, 431 (1-2), 315–321. doi: <https://doi.org/10.1016/j.msea.2006.06.023>
52. Christiansen, T. L., Hummelshøj, T. S., Somers, M. A. J. (2010). Expanded austenite, crystallography and residual stress. *Surface Engineering*, 26 (4), 242–247. doi: <https://doi.org/10.1179/026708410x12506870724316>
53. Kartikasari, R., Subardi, A., Wijaya, A. E. (2021). Development of Fe-11Al-xMN alloy steel on cryogenic temperatures. *Eastern-European Journal of Enterprise Technologies*, 5 (12 (113)), 60–68. doi: <https://doi.org/10.15587/1729-4061.2021.243236>
54. Zhou, R., Northwood, D. O., Liu, C. (2020). On nitrogen diffusion during solution treatment in a high nitrogen austenitic stainless steel. *Journal of Materials Research and Technology*, 9 (2), 2331–2337. doi: <https://doi.org/10.1016/j.jmrt.2019.12.064>